

The Crystallization Kinetics of Filled Poly(ethylene terephthalate)

SEN CHENG and ROBERT A. SHANKS*

Applied Chemistry, Royal Melbourne Institute of Technology, Melbourne, Australia

SYNOPSIS

The crystallization kinetics of poly(ethylene terephthalate) was measured under isothermal conditions by DSC in the presence of various fillers and with varying filler concentrations. The fillers used were carbon, titanium dioxide, glass fiber, and calcium carbonate. The kinetics was calculated using the slope of the crystallization vs. time plot, the times for 10% and 50% reduced crystallization, and the Avrami equation. Activation energies were determined from measurements under different isothermal temperatures. The fillers caused athermal nucleation to be inhibited as shown by the increased values of the Avrami exponent, n . Interactions between the polyester and filler were interpreted to reduce the mobility of the polymer in the melt. This decreased the rate of crystallization and increased its activation energy. The order of the filler effect in reducing crystallization was the following: no filler < carbon < titanium dioxide < glass fiber < calcium carbonate. The concentrations of fillers were above those typically used for nucleation and more in the range expected for reinforcement or dilution of the polymer. © 1993 John Wiley & Sons, Inc.

INTRODUCTION

The effect of filler on the crystallization kinetics of poly(ethylene terephthalate) (PET) was expected to be influenced by the reduction in mobility resulting from adsorption of the polymer onto the surface of the filler, though nucleation may have been important. The effect of filler can be related to both the potential for formation of a nucleus of critical size (nucleation) and to the activation energy for transfer of polymer across the melt-crystal interface (growth). Increase in the filler content can cause a larger number of macromolecules to become adsorbed by the filler and, hence, decrease their mobility. Athermal nucleation may be observed when heterogeneous particles initiate crystal growth. Thermal nucleation is homogeneous nucleation, where the nucleation rate is often assumed to be constant. In practice, nucleation is often intermediate between these two limits.

Fillers of different natures may differ in the

strength of their adsorption of polymer molecules. Small particle-size fillers may be the center of a spherulite. Fillers whose particle size is large in comparison with the core of the spherulite cannot form the center of spherulites. In this latter case, it is the actual surface of the particles that may influence nucleation. The filler may also influence the size distribution of the spherulites.

It is known that crystallization kinetic parameters depend on the temperature of crystallization. When crystallization from the melt occurs, the temperature for the maximum rate of crystallization decreases when smaller nuclei are formed or when the concentration of chain units for nucleation is lower. The purpose of the work described in this paper was to study the effect of filler on crystallization of PET. Of the techniques available for study of crystallization, DSC was chosen because a relatively small sample size can be used, thereby enabling more rapid thermal equilibration.¹ The DSC technique can be used in two ways to study crystallization—*isothermal* and *temperature scanning* (nonisothermal or dynamic mode). The isothermal mode was used in this study as it is more suitable for evaluating the kinetic parameters of crystallization.²

* To whom correspondence should be addressed.

EXPERIMENTAL

1. Materials

1.1. Poly(ethylene terephthalate)

Samples of PET were obtained in thin sheet form from Cadillac Plastics (Australia). The limiting viscosity number was measured in phenol-*o*-dichlorobenzene solution (60:40 by mass) at 25°C as 63 mL/g.

1.2. Fillers

The following fillers were used in all the studies carried out in this project. They were characterized by measuring their mean particle diameters using scanning electron microscopy:

Carbon black (ACARB SCF)	60 μm
Titanium dioxide (rutile, Tioxide Aust)	70 μm
Glass fibre (of mean length 1.0 mm)	90 μm
Calcium carbonate (whiting)	110 μm
Kaolin	50 μm

1.3. Preparation of Filled Polyesters

PET was fused at 280°C and then the filler was added and intimately mixed. The samples were then pressed into uniform sheets approximately 1 mm thick using a hydraulic press at 280°C under a pressure of 3 kg/cm² for 5 min. The samples were then slowly cooled to room temperature.

2. Procedures

2.1. Calibration of the DSC Instrument

The DSC was calibrated using high-purity indium. Indium has a melting temperature of 156.4°C and an enthalpy of fusion of 28.40 J/g (6.79 cal/g). A mass of 5–10 mg was used for each indium sample. The DSC was run at either 10 or 20°C/min. The temperature scale was calibrated by measuring the peak temperature of the indium melting endotherm and found to be correct to within the readability of the temperature thermocouple trace ($\pm 0.5^\circ\text{C}$).

2.2. Isothermal Crystallization

The kinetics of isothermal crystallization were measured by heating each sample to 280°C for 8 min to ensure complete melting. The DSC was then cooled as fast as possible (about 100°C/min) to the desired isothermal crystallization temperature. The

crystallization exotherm was recorded as a function of time. The DSC conditions used were the following: sensitivity = ± 2 mcal/s and sample mass of about 10 mg precisely weighed.

Integrations across each exotherm were used to construct plots of reduced fraction of crystallinity vs. time. The linear section of this plot was used to calculate a rate of crystallization. Arrhenius equation correlation of such rates, determined from isothermal crystallizations measured at different temperatures, were used to calculate thermodynamic parameters. The times to reach 0.1 ($t_{0.1}$) and 0.5 ($t_{0.5}$) of the limiting crystallization were also measured. Analysis of the data was also performed by fitting the data to the Avrami equation. The Avrami rate coefficient and exponent were obtained from this analysis. The data deviated from the Avrami equation at high values of reduced crystallinity. These data were not included in the final computer analysis. The area under the whole melting endotherm was used to calculate the crystallinity of the samples.

2.3. Experimental Uncertainty

The deviations in the rate of crystallization and the crystallization kinetic parameters over the temperature range 216–224°C were, on average, 10%, e.g., $0.010 \pm 0.001 \text{ s}^{-1}$. The deviation in the corresponding crystallinity averaged 5% or, e.g., $28.1 \pm 1.5\%$.

RESULTS AND DISCUSSION

1. Isothermal Crystallization of Filled PET

Typical isothermal DSC curves for the crystallization of filled PET are shown in Figure 1. The position of the maxima and the breadth of the curves varies considerably with crystallization temperature. Under constant crystallization temperature, the crystal growth rate was proportional to time.

The area under the crystallization exotherm can be used to calculate the reduced crystallinity at a particular time. The mass fraction of crystalline material, $x_{(t)}$, at time, t , can be calculated from

$$x_{(t)} = a/A \quad (1)$$

where a is the area under the DSC curve from $t = 0$ to $t = t$, and A , the total area under the crystallization curve. Since no polymer ever becomes 100% crystalline, this is referred to as the reduced crystallinity. The reduced crystallinity was a function of time as is shown by the plots in Figures 2 and 3.

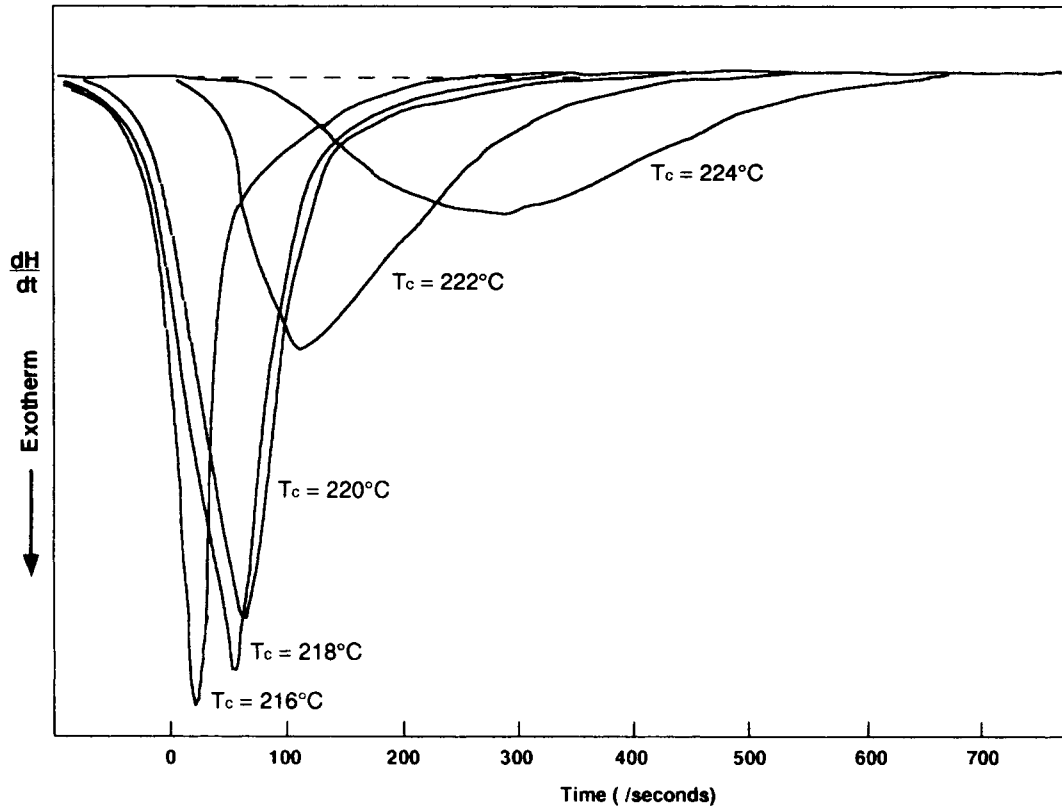


Figure 1 Isothermal DSC for crystallization of PET-TiO₂-1-1.

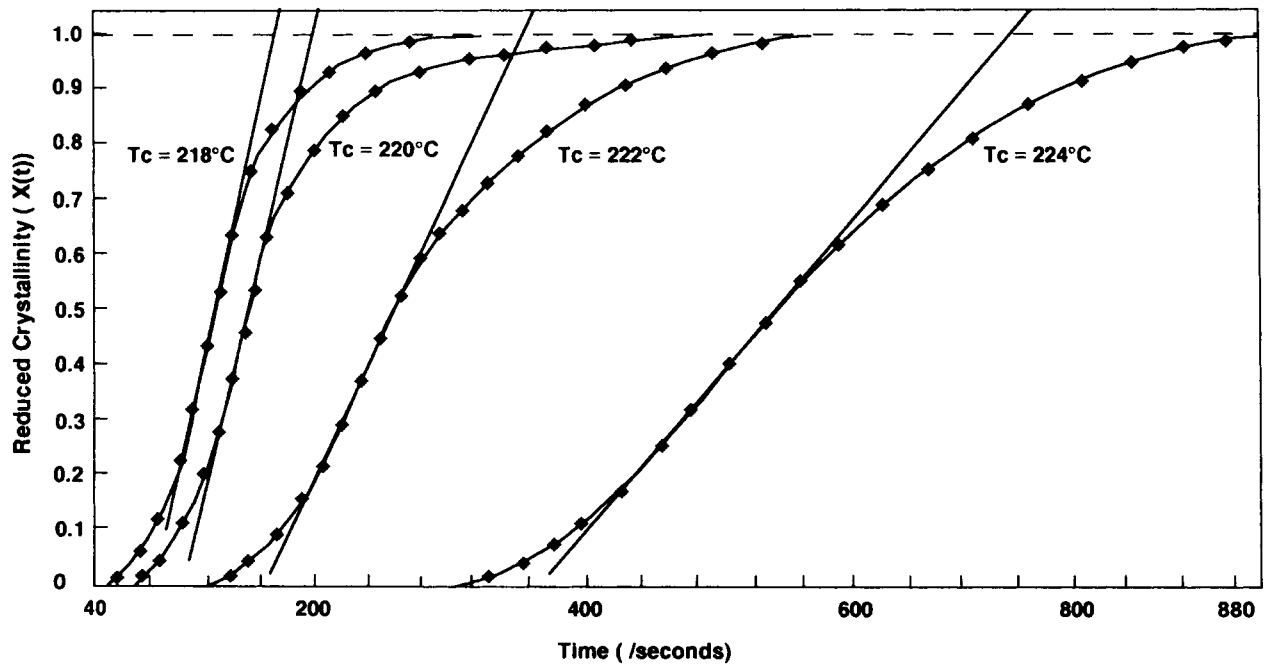


Figure 2 Reduced crystallinity as a function of time plot for PET-TiO₂-1-1.

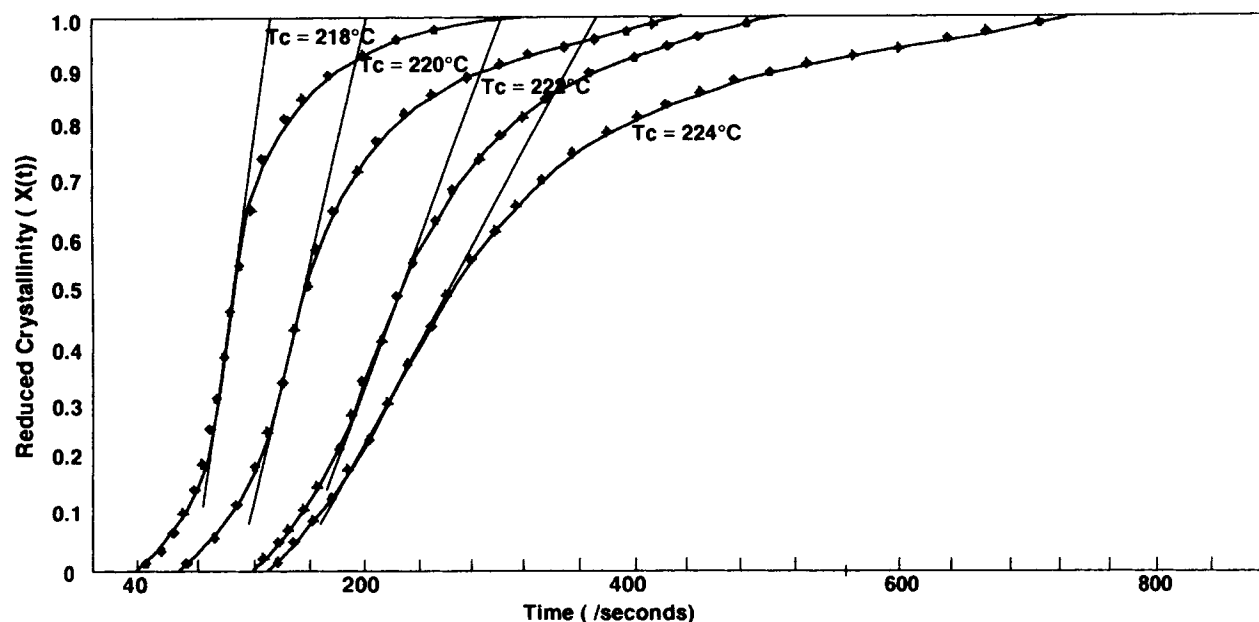


Figure 3 Reduced crystallinity as a function of time plot for PET-ACARB-1-1.

Initially, the crystallization was controlled by nucleation and there was a delay after which the rate increased. The crystallization rate became constant and the plot became linear for the midperiod of the crystallization. As the radii of the spherulites impinged on each other and the material still available for crystallization diminished, the rate decreased and the equilibrium crystallinity was approached more slowly. The slope of the linear region of a plot of $x(t)$ vs. t is a measure of the rate of crystallization.³ In addition, the times for the reduced crystallinity to reach 0.1 ($t_{0.1}$) and 0.5 ($t_{0.5}$) of the final crystallinity were calculated.

The activation energy associated with the process of crystallization has been evaluated using the Arrhenius equation on measurements made at a number of temperatures:

$$k_c = A \exp(-E_{\text{act}}/RT_c) \quad (2)$$

where k_c is the rate coefficient for crystallization; A , the Arrhenius collision frequency; E_{act} , the Arrhenius activation energy; T_c , the crystallization temperature, and R , the gas constant. Absolute reaction rate theory was then used to derive the thermodynamic parameters: changes in enthalpy, entropy, and Gibbs' free energy.

The kinetic analysis was carried out using the Avrami equation:

$$\phi(t) = 1 - x(t) = \exp(-kt^n) \quad (3)$$

where $\phi(t)$ is the mass of uncrystallized material at time t ; k , the rate coefficient, and n , a constant that depends on both the nucleation and growth of the crystals. The Avrami equation assumes that growth ceases at the onset of the impingement between growing crystals, and n is usually given integral values to permit theoretical interpretation. The measurements only followed the Avrami equation to about 0.8 crystallization, probably because of this latter constraint.

The rate coefficient was also calculated from the half-life for crystallization, $t_{0.5}$, using the equation

$$k' = \ln(2)/t_{0.5}^n \quad (4)$$

Computer programs were written to perform all the calculations and to calculate the correlation coefficient and standard deviation for each of the data fits. The results of these analyses of the data are listed in Tables I and II.

The rate of crystallization is strongly dependent on temperature. As the temperature is decreased, i.e., the supercooling ($\Delta T = T_m^0 - T_c$, where T_m^0 is the equilibrium melting temperature and T_c is the crystallization temperature) is increased, the rate of crystallization increases. For example, for the sample PET-0-2 (unfilled PET, sample no. 2), as the crystallization temperature decreased from 218 to 216°C, i.e., by only 2°C, the rate of crystallization was increased 1.6 times. For the sample PET-TiO₂-

Table I Effect of Filler Type on Isothermal Crystallization Kinetics

Sample	T_c (°C)	k_c (s ⁻¹)	$t_{0.5}$ (s)	$t_{0.1}$ (s)	k (s)	n	k' (s)	C (%)	E_{act} (kJ/mol)	$\ln A$ (s)
PET-0-2	216	0.0160	54	29	1.6E-05	2.7	1.6E-05	28	257	67
	218	0.0100	106	59	2.0E-06	2.7	1.9E-06	28		
	220	0.0082	141	85	1.4E-07	3.1	1.4E-07	25		
	222	0.0073	193	128	4.4E-09	3.6	4.4E-09	—		
PET-ACARB-1-1	218	0.0094	114	66	8.2E-07	2.9	8.2E-07	27	275	72
	220	0.0072	—	—	1.8E-08	3.4	1.8E-08	26		
	222	0.0054	228	155	1.6E-09	3.7	1.6E-09	25		
	224	0.0042	263	167	2.1E-10	4.0	1.9E-10	24		
PET-TiO ₂ -1-1	216	0.0121	76	43	3.3E-06	2.8	3.3E-06	27	394	101
	218	0.0083	126	78	2.4E-08	3.5	2.5E-08	26		
	220	0.0068	149	99	7.8E-09	3.7	7.8E-09	24		
	222	0.0048	256	172	4.6E-10	3.8	4.5E-10	23		
	224	0.0023	534	358	2.3E-11	3.8	2.3E-11	23		
PET-glass-1-1	218	0.0082	131	83	7.8E-09	3.8	7.9E-09	25	524	133
	220	0.0066	—	—	4.4E-09	3.8	4.4E-09	23		
	222	0.0042	276	180	1.8E-10	3.9	1.7E-10	23		
	224	0.0017	692	456	4.0E-12	3.9	4.2E-12	23		
PET-CaCO ₃ -1-1	218	0.0081	132	84	7.5E-09	3.8	7.0E-09	24	525	134
	220	0.0038	243	137	3.6E-09	—	3.2E-09	23		
	222	0.0028	456	311	1.8E-11	4.0	1.8E-11	22		
	224	0.0016	785	552	2.0E-12	4.0	2.0E-12	21		

Table II Effect of Filler Level on Isothermal Crystallization Kinetics

Sample	T_c (°C)	k_c (s ⁻¹)	$t_{0.5}$ (s)	$t_{0.1}$ (s)	k (s)	n	k' (s)	C (%)	E_{act} (kJ/mol)	$\ln A$ (s)
PET-0-2	216	0.0160	54	29	1.6E-05	2.7	1.6E-05	28	257	67
	218	0.0100	106	59	2.0E-06	2.7	1.9E-06	28		
	220	0.0082	141	85	1.4E-07	3.1	1.4E-07	25		
	222	0.0073	193	128	4.4E-09	3.6	4.4E-09	—		
PET-TiO ₂ -1-1	216	0.0121	76	43	3.3E-06	2.8	3.3E-06	27	394	101
	218	0.0083	126	78	2.4E-08	3.5	2.5E-08	26		
	220	0.0068	149	99	7.8E-09	3.7	7.8E-09	24		
	222	0.0048	256	172	4.6E-10	3.8	4.5E-10	23		
	224	0.0023	534	358	2.3E-11	3.8	2.3E-11	23		
PET-TiO ₂ -5-1	216	0.0095	108	66	2.5E-07	3.2	2.5E-07	23	575	146
	218	0.0073	162	107	3.0E-09	3.8	3.0E-09	22		
	220	0.0034	265	148	2.9E-09	3.5	2.3E-09	20		
	222	0.0018	718	499	6.8E-12	3.9	6.8E-12	20		
PET-TiO ₂ -10-1	216	0.0084	128	80	4.5E-08	3.4	4.5E-08	23	665	168
	218	0.0062	193	129	1.7E-09	3.8	1.7E-09	22		
	220	0.0025	245	157	6.8E-10	3.8	6.5E-10	19		
	222	0.0013	1006	687	2.4E-12	3.8	2.4E-12	18		

1-1 (PET sample no. 1, containing 1% TiO_2 filler), as the crystallization temperature decreased from 220 to 216°C, i.e., by only 4°C, the rate of crystallization was increased by 1.8 times.

The rate of crystallization was decreased as the level of filler increased; as the level of TiO_2 increased from 0 to 5%, the rate of crystallization decreased sharply. A further increase to 10% filler produced a more gradual decrease in rate for various ΔT (see Table II and Fig. 4). Though the effect of the fillers was not the same, each caused a decrease in the crystallization rate (see Table I). This filler effect is related to both the potential for formation of a nucleus of critical size and to the activation energy for transfer across the melt-crystal interface. Increase in the filler content is accompanied by transition of an apparent ever-larger number of macromolecules into the boundary layers, in which their mobility decreases, so this results in a very strong influence on the rate of crystallization. Equation (2) summarizes the influence of the two effects on the overall rate of crystallization, k_c .⁴⁻⁶

In the region where the temperature is close to the melting temperature, the rate of crystallization is controlled by nucleation. This may be evidence for a change in ΔG for the formation of a nucleus of critical size. In such a case, the effect of filler will be less important because ΔG is the predominant factor.⁷ In crystallization from the viscoelastic state

(heating from an initial temperature below the glass transition temperature), since ΔE is the predominant factor in controlling the crystallization process, an increase in filler would cause an increase in viscosity and give rise to a decrease in the rate of crystallization.⁸

Values of the times for 10% and 50% of the final reduced crystallization, $t_{0.1}$ and $t_{0.5}$, are also listed in Tables I and II. The $\log(t_{0.5})$ dependence on the TiO_2 filler content for various supercooling temperatures (ΔT) is shown in Figure 5. The values of $t_{0.5}$ are in the linear region of the rate plots and so are related to the crystallization rate. These half-times were used to calculate a value for the rate coefficient, k' , which could be compared with the value obtained from the slope. The $t_{0.1}$ values are more reflective of the initial nucleation period where the rate of crystallization was still approaching the steady-state value.

Thermodynamic parameters were calculated from the Arrhenius equation (2).⁹⁻¹² The E_{act} value for unfilled PET is very close to other data previously reported, e.g., Baer¹³ reported 267.5 kJ/mol and Vilanova et al.¹ reported 273.7 kJ/mol for medium molar mass PET. The addition of filler, in general, leads to an increase in E_{act} , although a low level of filler (1% TiO_2) gave a lower value for E_{act} , whereas higher levels gave higher values for E_{act} and, hence, a decrease in rate of crystallization (Table II). The

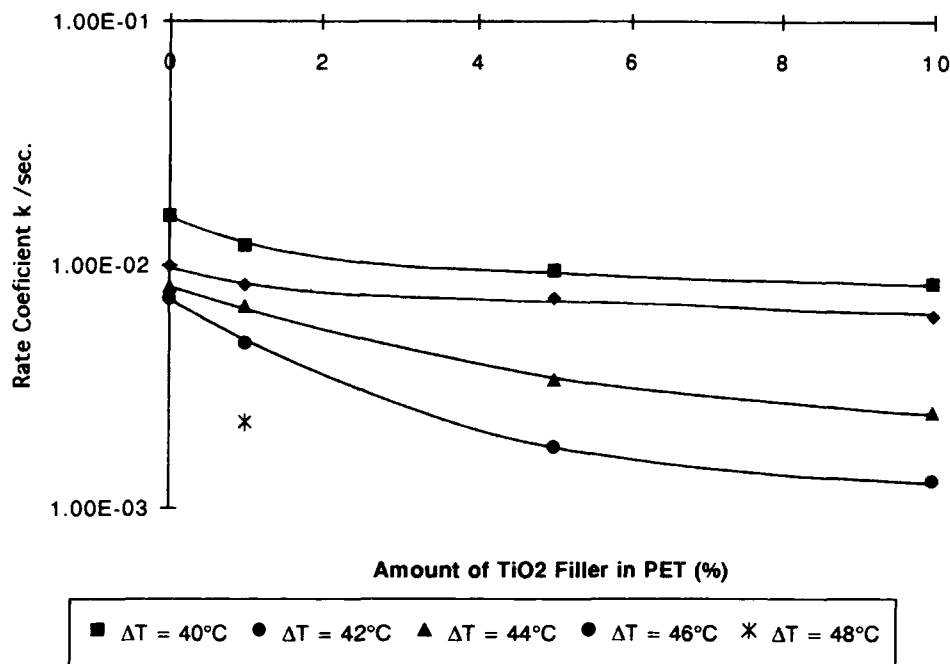


Figure 4 The rate of crystallization dependence on the amount of TiO_2 for various ΔT .

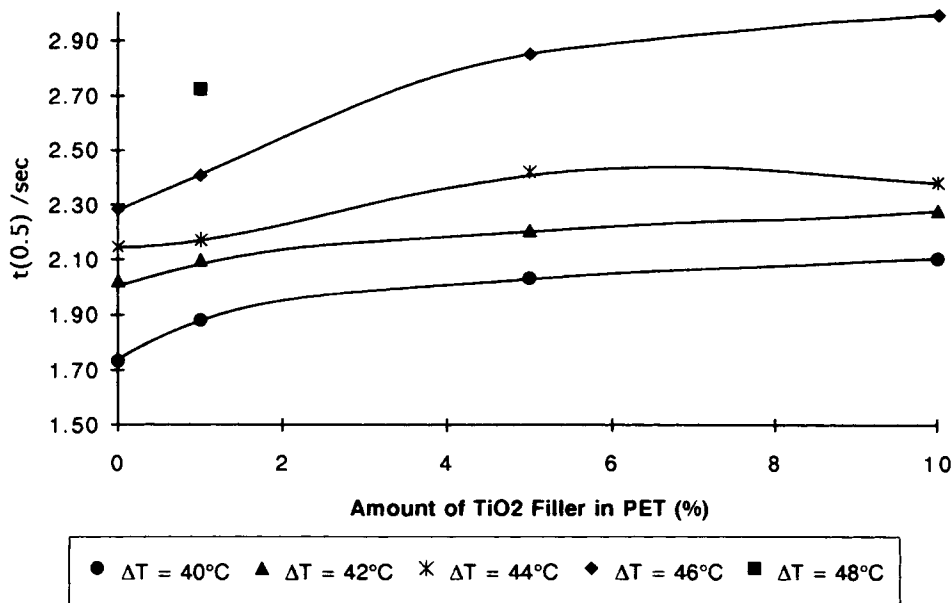


Figure 5 The log $t_{0.5}$ dependence on the amount of TiO_2 filler in PET for various ΔT .

different filler types show different changes in activation energy. Carbon gave a small increase in E_{act} , whereas the other fillers, especially glass fibers and CaCO_3 , produced larger increases (Table I).

The crystallization mechanism of unfilled PET should be similar to other polymers, such as polycaprolactone¹⁴ and poly(ethylene oxide).¹⁵ The presence of filler is postulated to produce distinct changes in the dynamics of this mechanism. There is a reduction in the mobility of the macromolecules due to their adsorption onto the filler, leading to an increased activation energy for crystallization.¹⁶ This effect increases with the proportion of filler. The Arrhenius collision frequency, A , includes two factors: the probability of collision or steric factor and the collision number.¹⁷ Both of these factors would be altered by adsorption onto a filler. As the filler content increases, the value of the collision parameter becomes higher. The values of the collision frequency are affected by the type of filler, with carbon producing only a small effect.

The data were also analyzed by the Avrami eq. (3). The influence of the Avrami rate coefficient (k) and exponent (n) on the shape of isothermal crystallization curves are shown in Figures 6–9. For the crystallization of PET, the Avrami exponent $n = 4$,¹⁸ indicating three-dimensional growth and dependence on homogeneous nucleation. As expected, the Avrami rate coefficients increase and the values for the Avrami exponent are decreased as the crystal-

lization temperature decreases. Fillers increase the Avrami exponent by a small amount, i.e., the process becomes more dependent on heterogeneous nucleation. The filler also diminished the crystallinity of the samples, probably by restricting movement of some molecules into crystallite formations. The crystallization does not follow the Avrami equation to completion. Taking logarithms of each side of the equation should give a linear plot (Figs. 6 and 7). The plots deviate from linearity at high crystallizations. The plots in Figure 8 are in agreement with the Avrami equation from 20 to 60% of the relative crystallinity. Other reports describe deviations from the Avrami equation.^{19,20}

Figure 9 shows the dependence of the rate coefficient on the TiO_2 filler content for PET at various supercooling temperatures. As shown by the simple kinetic analysis of the data, as the filler content increases, the rate coefficient decreases. Figure 10 shows the corresponding dependence of the Avrami exponent on the TiO_2 filler content. As the filler content increases, so the value of n increases, though leveling out for higher filler contents. The values of k and n are also dependent on the type of filler. For theoretical interpretation, the value of n is usually given integer values. The values observed in this work and other studies such as for polyethylene,^{21,22} poly(ethylene oxide),²³ and poly(ether ether ketone)²⁴ are noninteger. This is even observed for poly(decamethylene terephthalate), which con-

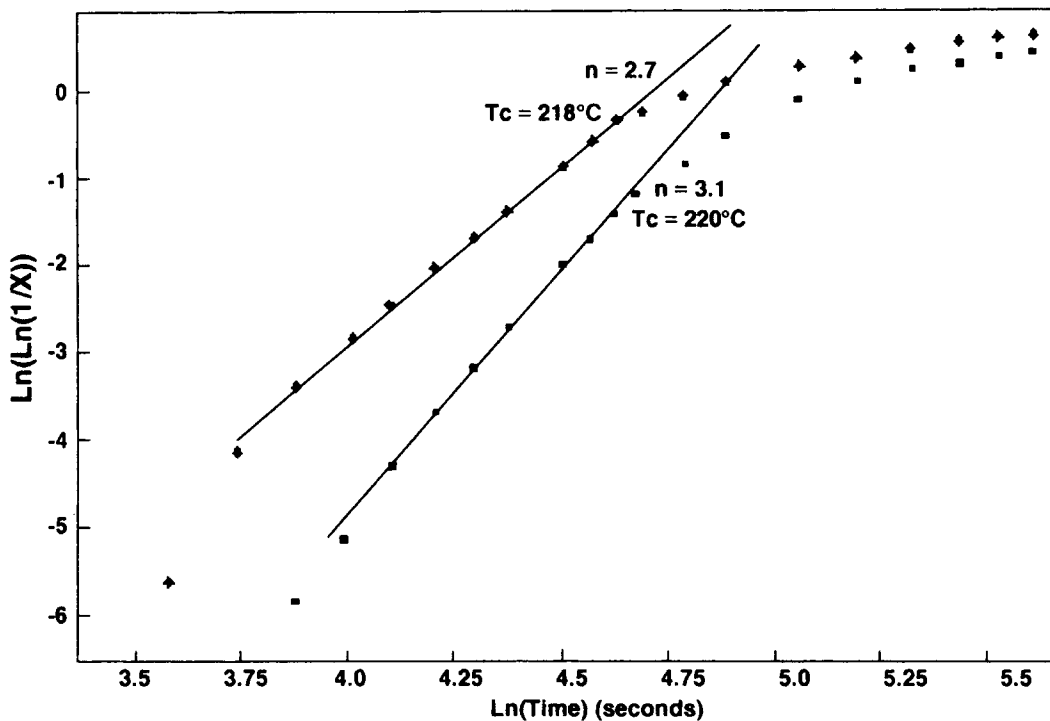


Figure 6 The Avrami equation for unfilled PET.

forms accurately to the Avrami equation for more than 95% of the crystallization process, yet $n = 3.59$.²⁵ This indicates that total dependence on a single nucleation mechanism is not usual. The het-

erogeneous and homogeneous nucleation mechanisms must be regarded as extreme models for the actual situation. Deviations can be caused by simultaneous and consecutive processes. In the former

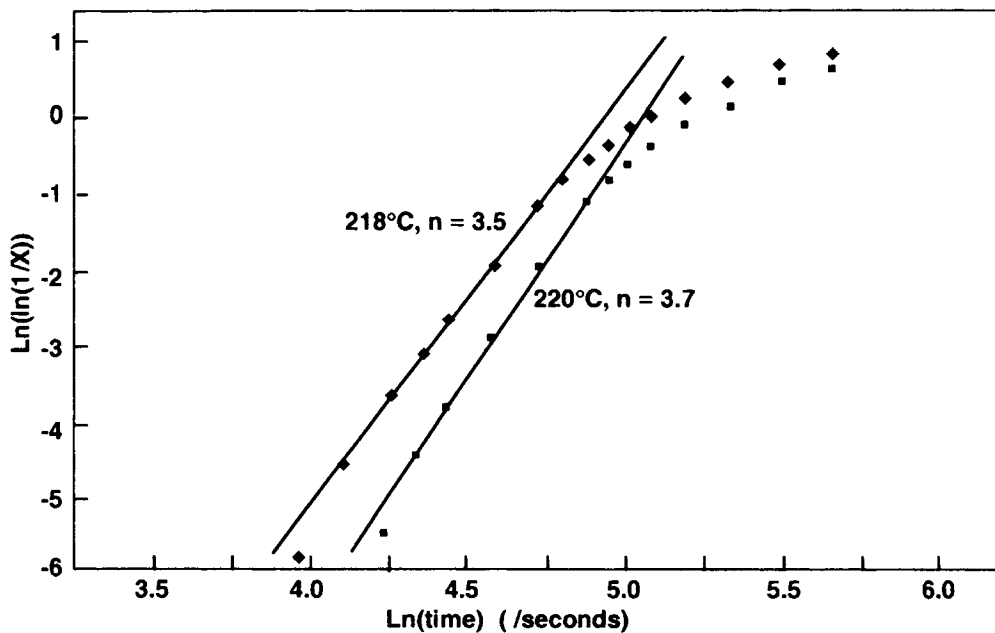


Figure 7 The Avrami equation for 1% TiO₂-filled PET.

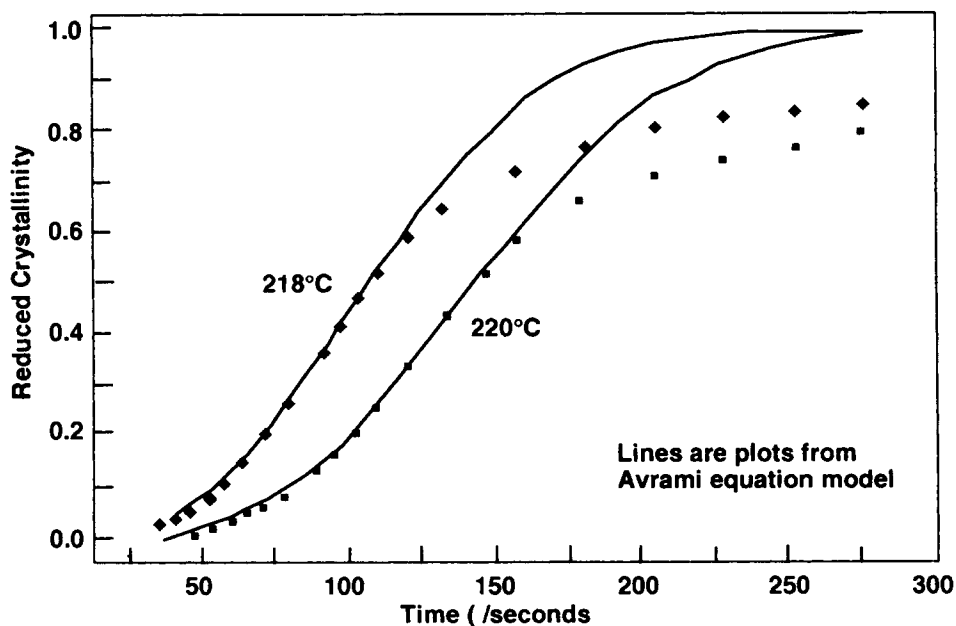


Figure 8 The deviation from the Avrami equation for isothermal crystallization of PET-0-2.

case, the simultaneous growth of two different types of spherulites may occur. Consecutive processes can occur when, e.g., when spherulitic growth starts from a rodlike or platelike nucleus. These cases can lead to a situation where the apparent value of n is changing during the crystallization.

2. Determination of the Crystallinity

The crystallinity was determined immediately after the isothermal crystallization by heating the sample and obtaining its melting endotherm. The enthalpy of fusion of the sample was calculated and used to

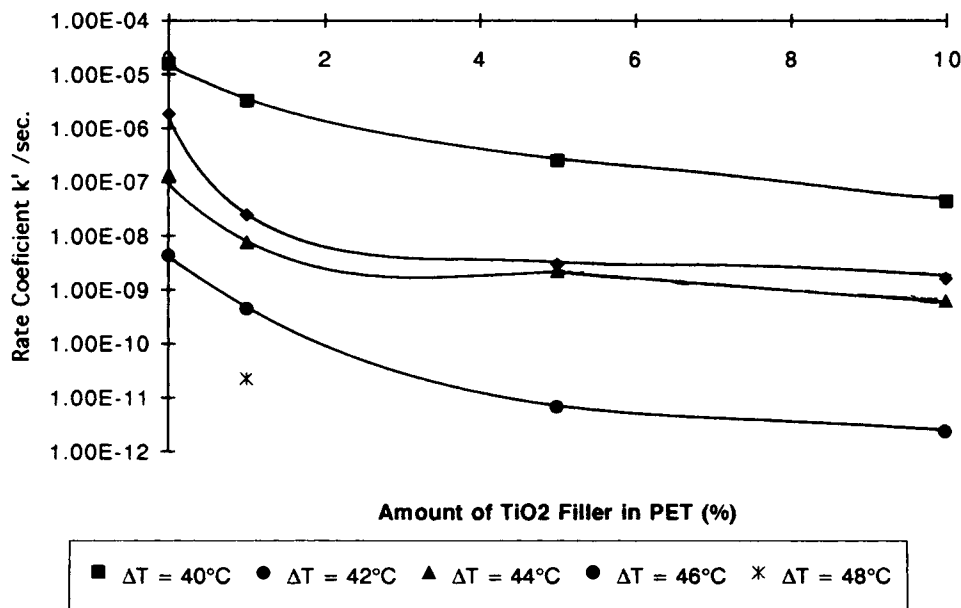


Figure 9 The rate coefficient of crystallization dependence on the amount of TiO_2 filler in PET for various ΔT .

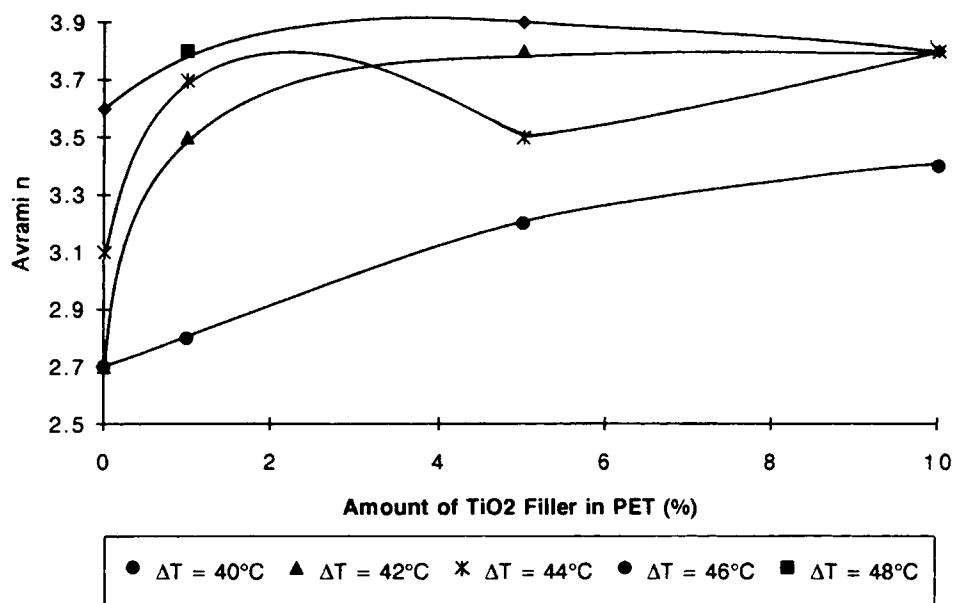


Figure 10 The n value dependence on the amount of TiO_2 filler in PET for various ΔT .

determine the crystallinity according to the following equation^{26,27}:

$$C = \Delta H / \Delta H_f \quad (5)$$

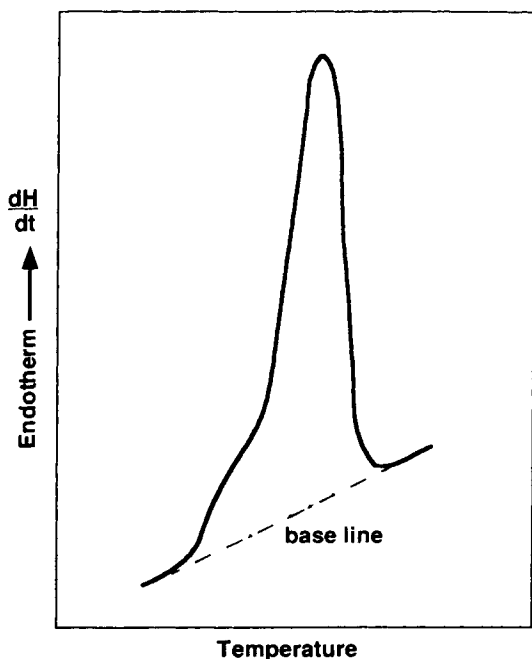


Figure 11 Melting endotherm of the crystals formed during isothermal crystallization at 218°C for 1% TiO_2 -filled PET.

where ΔH is the total enthalpy of melting of the sample and ΔH_f is for pure crystals of the polymer. Figure 11 shows the melting endotherm for PET containing 1% TiO_2 after isothermal crystallization at 218°C . From this endotherm, the enthalpy of fusion was calculated as 33.48 J/g . The value for the enthalpy of fusion of a pure crystal of PET was taken as $129.0 \pm 0.5 \text{ J/g}$,²⁸ although many widely varying values have been reported in the literature. Figure 12 and Tables I and II show the values of the crystallinity and their variation with TiO_2 content. When the filler content is low, the crystallinity exhibits a rapid decrease, which levels out for higher filler levels. Table I shows the effect of different types of filler on the crystallinity. Each of the fillers decreases the crystallinity, with carbon, as in the crystallization kinetic study, having the least effect.

CONCLUSION

The effect of fillers on the crystallization of poly(ethylene terephthalate) has been studied by differential scanning calorimetry (DSC). Although the kinetics have been studied under several conditions, those reported refer to isothermal conditions after cooling from the melt. These conditions enable the effect of filler on nucleation to be determined using the Avrami equation. The kinetics of the crystallization process were described by the Avrami

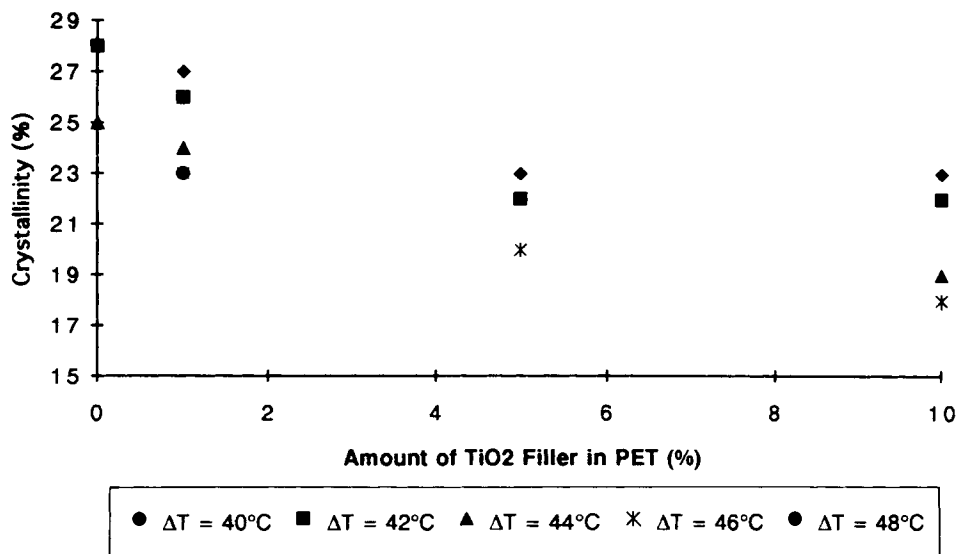


Figure 12 The crystallinity dependence on the amount of TiO₂ filler in PET for various ΔT .

equation. This equation takes into account the two stages of crystallization: nucleation and growth. The nucleation kinetics is in its limits athermal or thermal. In the first case, a fixed number of nuclei start growing at the beginning with no additional nuclei forming at a later time, giving a lower value of n . In the second case, new nuclei are forming throughout the crystallization, giving a higher value of n . The fillers caused athermal nucleation to be inhibited, as shown by the increased values of the Avrami exponent, n . Interactions between the polyester and filler were interpreted to reduce the mobility of the polymer in the melt. This decreased the rate of crystallization and increased its activation energy.

Decreasing the crystallization temperature increased the rate of crystallization, decreased $t_{0.1}$ and $t_{0.5}$ of crystallization, increased the Avrami rate coefficient, decreased the Avrami exponent, and increased the crystallinity. Increasing the concentration of a filler (titanium dioxide) decreased the rate of crystallization, increased $t_{0.1}$ and $t_{0.5}$ of crystallization, decreased the Avrami rate coefficient, increased the Avrami exponent, decreased the percent crystallinity, increased the activation energy for crystallization, and increased the Arrhenius collision parameter.

These observations are consistent with the main effect of the filler restricting molecular motions by adsorption of the macromolecules. Different types of filler such as carbon, titanium dioxide, glass fiber, and calcium carbonate produce similar effects. The

effects were strongest for the latter two and weakest for carbon. The order of the filler effect in reducing crystallization was the following: no filler < carbon < titanium dioxide < glass fiber < calcium carbonate.

REFERENCES

1. P. C. Vilanova, S. M. Ribas, and G. M. Guzman, *Polymer*, **26**, 423 (1985).
2. T. Sun, J. Pereira, and R. S. Porter, *J. Polym. Sci. Polym. Phys. Ed.*, **22**, 1163 (1984).
3. J. R. Knox, *Analytical Calorimetry*, Plenum Press, New York, 1968, Vol. 1, p. 45.
4. L. Mandelkern, *Crystallization of Polymers*, McGraw-Hill, New York, 1964, pp. 218-273.
5. L. Mandelkern, N. L. Iain, and H. Kim, *J. Polym. Sci. A-2*, **6**, 165 (1968).
6. V. G. Baranov, A. V. Kenarov, and T. I. Volkov, *J. Polym. Sci.*, **C-30**, 277 (1970).
7. L. Mandelkern, J. M. G. Fatou, and C. Howard, *J. Phys. Chem.*, **68**, 3386 (1964).
8. L. Mandelkern, J. M. G. Fatou, and C. Howard, *J. Phys. Chem.*, **69**, 956 (1965).
9. C. D. Craver, *Adv. Chem. Ser.* **203**, 237 (1983).
10. H. J. Borchardt and F. Daniels, *J. Am. Chem. Soc.*, **79**, 41 (1957).
11. R. A. Hill, *Nature*, **227**, 703 (1970).
12. M. D. Baro, N. Clavaguera, S. Bordas, M. T. Clavaguera-Mora, and J. Casas-Vazquez, *J. Therm. Anal.*, **11**, 273 (1977).

13. I. Baer, J. R. Collier, and D. R. Carter, *SPE Trans.*, **5**, 22 (1965).
14. R. Perret and A. Skoulios, *Makromol. Chem.*, **156**, 157 (1972).
15. Y. Godovsky, G. L. Slonimsky, and N. M. Garbar, *J. Polym. Sci. Polym. Symp.*, **37**, 1 (1972).
16. Y. S. Lipatov, *Physical Chemistry of Filled Polymers*, Rubber and Plastics Association of Britain, Shawbury, England, Translation, 1979, pp. 41-59.
17. R. Chang, *Physical Chemistry with Application to Biological Systems*, McMillan, New York, 1977, p. 386.
18. A. Sharples, *Introduction to Polymer Crystallization*, Edward Arnold, London, 1966, p. 51.
19. M. Takayanagi, *Mem. Fac. Eng. Kyushu Univ. Jpn.*, **16**, 112 (1957).
20. K. R. Chynoweth and Z. H. Stachurski, *Polymer*, **27**, 1912 (1986).
21. W. Banks, M. Gordon, R. J. Roe, and A. Sharples, *Polymer*, **4**, 61 (1963).
22. W. Banks and A. Sharples, *Macromol. Chem.*, **59**, 233 (1963).
23. I. H. Hillier, *J. Polym. Sci. A-2*, **3**, 3067 (1965).
24. P. Cebe and S. D. Hong, *Polymer*, **27**, 1183 (1986).
25. W. Banks, J. N. Hay, and A. Sharples, *J. Polym. Sci. A-2*, **2**, 4059 (1964).
26. R. L. Miller, *Encycl. Polym. Sci. Technol.*, **4**, 487 (1966).
27. A. P. Gray, *Perkin-Elmer Therm. Analy. Newsl.*, 24 (1975).
28. M. S. Yagpharov, *J. Therm. Anal.*, **23**, 120 (1982).

Received April 7, 1992

Accepted May 18, 1992